Geomechanics and Engineering, *Vol. 29, No. 3 (2022) 331-338*
https://doi.org/10.12989/gae.2022.29.3.331

Reliability analysis of tunnel face stability considering seepage effects and strength conditions

Jun Kyung Park*

Department of Civil and Environmental Engineering, Daelim University College, Anyang, Gyeonggi Province, 13916, Republic of Korea

(Received December 17, 2021, Revised February 23, 2022, Accepted March 3, 2022)

Abstract. Face stability analyses provides the most probable failure mechanisms and the understanding about parameters that need to be considered for the evaluation of ground movements caused by tunneling. After the Upper Bound Method (UBM) solution which can consider the influence of seepage forces and depth-dependent effective cohesion is verified with the numerical experiments, the probabilistic model is proposed to calculate the unbiased limiting tunnel collapse pressure. A reliability analysis of a shallow circular tunnel driven by a pressurized shield in a frictional and cohesive soil is presented to consider the inherent uncertainty in the input parameters and the proposed model. The probability of failure that exceeding a specified applied pressure at the tunnel face is estimated. Sensitivity and importance measures are computed to identify the key parameters and random variables in the model.

Keywords: face stability; importance measures; probabilistic model; reliability analysis; sensitivity; UBM

1. Introduction

Face stability analyses are required to determine the proper pressure to be used for pressurized shield construction of shallow circular tunnels. Analytical, limit based methods have been developed (Atkinson and Potts 1977, Davis *et al.* 1980) to calculate the optimum supporting pressure, which avoids face collapse (active failure) and surface 'blow-out' (passive failure). Active failure of the tunnel face is caused by surcharge and self-weight exceeding the frictional resistance and tunnel face pressure. Under passive conditions, the roles are reversed and the face pressure causes blow-out with resistance being provided by the surcharge, frictional resistance, and self-weight. Three failure mechanisms which involve the movement of solid conical blocks with circular cross sections, proposed by Leca and Dormieux (1990), are shown in Fig. 1. M1 and M2 failure mechanisms are single-cone and dual-cone systems, respectively; where the cones move into the excavation. An M3 failure mechanism is a single-cone, passive mechanism, where the cone moves outward to the surface.

In this study, the M2 collapse failure mechanism, which is most common failure pattern in shield tunneling (Chambon and Corte 1994), is investigated by the upper-bound theorem. Park (2011) proposed the general solutions for the limiting tunnel collapse pressure in a Mohr-Coulomb (c', Ø') soil which combine the depth-dependence of effective cohesion of normally consolidated clays and the influence of seepage.

*Corresponding author, Assistant Professor
E-mail: jkpark0215@daelim.ac.kr

The stability analysis of tunnels and the computation of soil displacements due to tunnelling were commonly performed using deterministic approaches (Jardine *et al.* 1986, Yoo 2002; Mroueh and Shahrour 2003, Wong *et al.* 2006, Eclaircy-Caudron *et al.* 2007, Khezri *et al.* 2016, Huang *et al.* 2021, Zhang *et al.* 2021). A reliability-based approach for the analysis of tunnels is more rational since it enables one to consider the inherent uncertainty in the input parameters and the models (Mollon *et al.* 2009, Binghua Zhou *et al.* 2020, Pan *et al.* 2021, Li *et al.* 2021). In this study, a reliability-based analysis of a shallow circular tunnel driven by a pressurized shield in a Mohr-Coulomb soil is presented. After the UBM solution is verified with the numerical experiments using FLAC^{3D}, the probabilistic model that accurately predicts the limiting tunnel collapse pressure and account for all the prevailing uncertainties is proposed. As an application, a reliability analysis of a shallow circular tunnel driven by a pressurized shield is presented to consider the inherent uncertainty in the input parameters and the proposed model. The developed probabilistic model is used to assess the conditional probability (fragility) of exceeding a specified applied pressure at the tunnel face threshold. Sensitivity and importance measures are carried out to identify the contribution of the random variable(s) to the reliability of the tunnel face stability.

2. Face stability analysis

2.1 Upper bound solutions

The M2 active failure state can be idealized by considering a circular rigid tunnel of diameter (D) driven under a depth of cover (C) in soil with an effective

ISSN: 2005-307X (Print), 2092-6219 (Online)

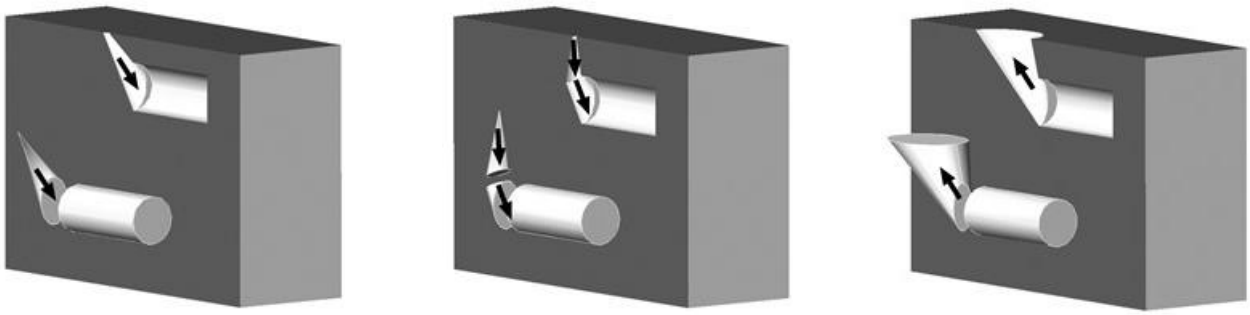

(a) M1 (b) M2 (c) M3

Fig. 1 Failure mechanisms of shield tunnel

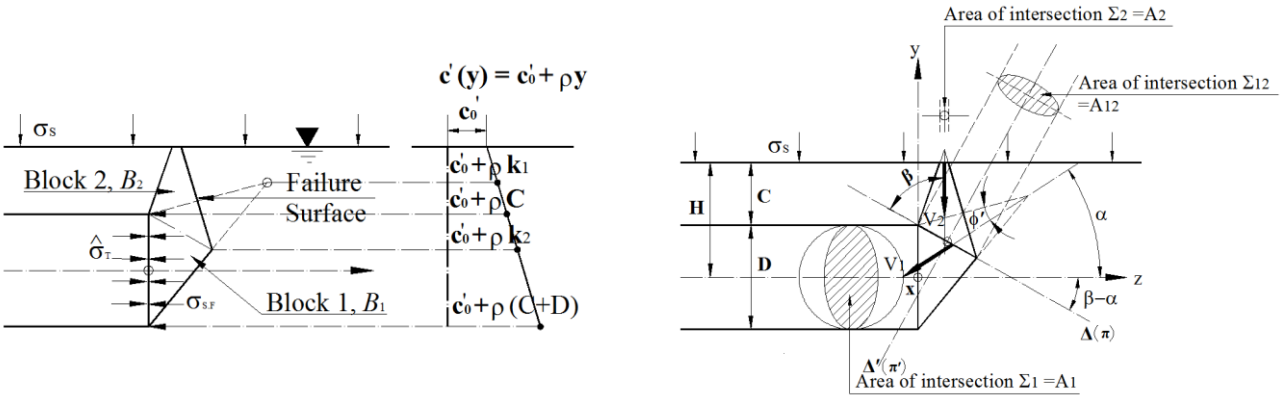

(a) Schematic cross-section (b) M2 failure mechanism

Fig. 2 Collapse mechanism of tunnel face by the two conical blocks

cohesion (c') increasing at rate (ρ) with depth. A surcharge (σ_s) is applied at the ground surface and a constant retaining pressure ($\hat{\sigma}_T$) is applied to the tunnel face. Fig. 2(a) shows a schematic cross-section of the M2 failure mechanism geometry.

Kinematically admissible failure mechanisms must be considered to obtain upper-bound solutions, initially developed by Leca and Dormieux (1990). An M2 failure occurs as two conical blocks move vertically and into the tunnel face, as shown in Fig. 2(b).

The required supporting pressure $\hat{\sigma}_T$ for Mohr-Coulomb soil is summarized in Eq. (1) (Park 2011).

$$\hat{\sigma}_T = \frac{\left[N_S Q_S + N_\gamma Q_\gamma - \frac{\sin\emptyset'}{\cos\alpha}\frac{R_F R_C^2}{R_A} - 1\right]\sigma_C + \sigma_{S.F.}}{(K_P - 1)} \quad (1)$$

where, R_A, R_C, R_F are simplified geometric coefficients, loading parameters (Q_S, Q_γ) and the coefficients (N_S, N_γ) are given in Eqs. (2)-(10).

$$R_A = \frac{[\cos(\alpha - \emptyset')\cos(\alpha + \emptyset')]^{1/2}}{\cos\emptyset'} \quad (2)$$

$$R_C = \frac{\cos(\alpha + \emptyset')}{\cos\emptyset'}\left[\frac{\sin(\beta - \emptyset')}{\sin(\beta + \emptyset')}\right]^{1/2} \quad (3)$$

$$R_F = \cos\emptyset' \cdot \left\{ \begin{array}{c} \left[\frac{\cos\alpha}{\sin\emptyset'}\frac{R_A}{R_C^2} - \cos(\alpha + \emptyset')\frac{R_D}{R_C}\right] \cdot \\ \rho(C + D - k_1) + \\ \left[\frac{\cos^2\emptyset' R_C R_D}{\cos(\alpha + \emptyset')} - \frac{R_E^2}{\sin\emptyset'\cos^2(\alpha + \emptyset')}\right] \cdot \\ \rho(k_2) + \\ \left[\frac{2\cos\beta\sin 2\emptyset'\cos(\alpha + \emptyset')}{\sin\beta}\frac{R_D^2}{R_C}\right] \cdot \\ \rho(k_2 - C) \end{array} \right\} \quad (4)$$

$$R_D = \frac{\sin\beta}{\sin\emptyset'\sin(\beta + \emptyset')} \quad (5)$$

$$R_E = \frac{\cos^2\emptyset'}{\cos(\alpha + \emptyset')}R_C^2 - \frac{2C}{D}\sin\emptyset' \quad (6)$$

$$Q_S = (K_P - 1)\frac{\sigma_S}{\sigma_C} + 1 \quad (7)$$

$$Q_\gamma = (K_P - 1)\frac{\gamma D}{\sigma_C} \quad (8)$$

$$N_S = \frac{1}{\cos\alpha\cos^2\emptyset'}\left[\frac{\sin(\beta - \emptyset')}{\sin(\beta + \emptyset')}\right]\frac{R_E^2}{R_A} \quad (9)$$

$$N_\gamma = \frac{1}{3}\left[\begin{matrix}\tan\alpha\, R_B + \dfrac{\cos\emptyset'\cos(\beta+\emptyset')}{2\sin\emptyset'\sin(\beta+\emptyset')}\dfrac{R_C^3}{R_A} - \\ \dfrac{1}{2\sin\emptyset'\cos\alpha\cos^2\emptyset'}\dfrac{\sin(\beta-\emptyset')}{\sin(\beta+\emptyset')}\dfrac{R_E^3}{R_A}\end{matrix}\right] \quad (10)$$

where, σ_C is the unconfined compressive strength, K_P is the Rankine passive earth pressure coefficient, $\sigma_{S.F.}$ is the seepage pressure acting on the tunnel face, γ is the unit weight of the soil, D is the tunnel diameter, k_1 is the apex of block 1, and k_2 is the lowest point of the intersection between B_1 and B_2.

The parameters in Eq. (1) correspond to geometry and Mohr-Coulomb soil properties except for the seepage pressure acting on the tunnel face. To calculate the seepage pressures acting on the tunnel face, the failure surface must be pre-determined from the limit analysis. Given this failure surface, seepage pressures acting on the tunnel face can be obtained from the difference of total head between the tunnel face and the failure surface. The average predicted seepage pressure is calculated using numerical analyses by FLAC^{3D}.

2.2 Numerical analysis of face stability using FLAC^{3D}

In order to investigate the behaviour of the tunnel face and to verify the UBM solutions, numerical analyses with the commercially available finite-difference code FLAC3D (FLAC^{3D} 2009) are carried out. In the numerical model, only one half is included due to symmetry condition. The model is sufficiently large to allow for any possible failure mechanism to develop and to avoid any influence from the boundary effects. The water table is assumed to be varied above the tunnel crown depending on the diameter of tunnel. In order to focus the analysis on the face failure in front of the shield machine, the excavation process was simulated using a simplified single-step excavation scheme, assuming that the tunnel is excavated 13 m (the general length of the shield machine) instantaneously. A uniform retaining pressure is applied to the tunnel face to simulate tunneling under compressed air. The highest pressure applied to the tunnel face for which soil collapse would occur is computed. This collapse pressure is the one for which the soil in front of the tunnel face undergoes downward movement. It is called the tunnel active pressure.

A circular tunnel of diameter $D = 5$ m and various cover depth C is driven in a Mohr-Coulomb soil is considered as shown in Fig. 3. The size of the numerical model is 20m in the X direction, 60m in the Z direction, and 40m in the Y direction.

These dimensions are chosen so as not to affect the value of the tunnel collapse pressure. A three-dimensional nonuniform mesh is used. The tunnel face region is subdivided into 100 separate zones since very high stress gradients are developed in that region. The bottom boundary is assumed to be fixed and the vertical boundaries are constrained in motion in the normal direction. A conventional elastic perfectly plastic model based on the Mohr-Coulomb failure criterion is adopted to represent the soil. The soil elastic properties employed are Young's

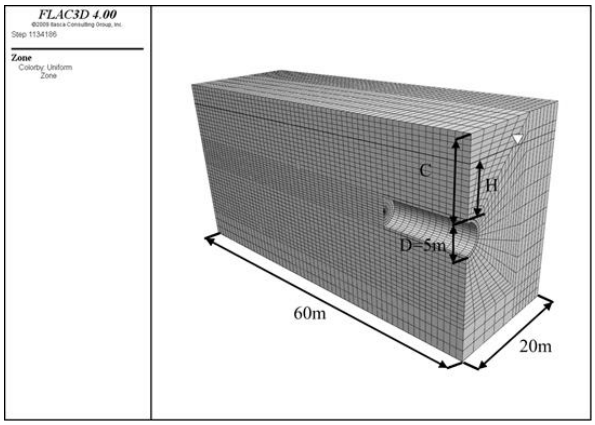

Fig. 3 Numerical mesh for the tunnel face stability in FLAC^{3D}

modulus, E =240 MPa and Poisson's ratio, ν =0.3. The value of the angle of internal friction and cohesion of the soil used in the analysis are $c_0' = 0{\sim}3$ kPa, $\phi' = 35^o$, $\rho =$ 0.1 kN/m^2/m and c_0' =variable, respectively. The soil unit weight is taken equal to 15.2 kN/m^3. It is noted that the soil elastic properties have a negligible effect on the collapse pressure. A concrete lining of 0.4m thickness is used in the analysis. The lining is simulated by a shell of linear elastic behavior. Its elastic properties are Young's modulus E =15 GPa and Poisson's ratio ν =0.2. The lining is connected to the soil via interface elements that follow Coulomb's law. The interface is assumed to have a friction angle equal to two-thirds of the soil angle of internal friction and cohesion equal to zero. Normal stiffness, $K_n = 10^{11}$ Pa/m and shear stiffness, $K_s = 10^{11}$ Pa/m are assumed to this interface. These parameters are a function of the neighboring elements rigidity and do not have a major influence on the collapse pressure. In terms of the fluid property, the porosity and permeability are assumed constant as 0.3 and 10^{-12}m$^2 \cdot$ sec/Pa, respectively. The fluid density is 9.8 kN/m^{3}and fluid bulk modulus assumed to be 2.0 GPa. For the computation of a tunnel collapse pressure using FLAC^{3D}, it is used a stress control method (Mollon *et al.* 2009). Fig. 4(a) shows the collapse velocity field given by FLAC^{3D}, and Fig. 4(b) shows the corresponding collapse displacement field at the time of failure. Stability against tunnel face collapse is ensured as long as the applied pressure ($\sigma_{applied}$) is greater than the tunnel collapse pressure (σ_T).

Steady-state flow occurs when at any point in a flow field the magnitude and direction of the flow velocity are constant with time. Transient flow occurs when at any point in a flow field the magnitude or direction of the flow velocity changes with time. The steady-state approach is valid as long as the water table is not drawn down by the existence of the tunnel. Steady-state groundwater flow condition is assumed in the analysis. There are two different types of the drainage condition during a tunnel construction such as the drainage type and the water-proof type. In the drainage type, ground water is drained through the tunnel wall as well as the tunnel face, while in the water-proof type drainage is allowed only through the tunnel face. After

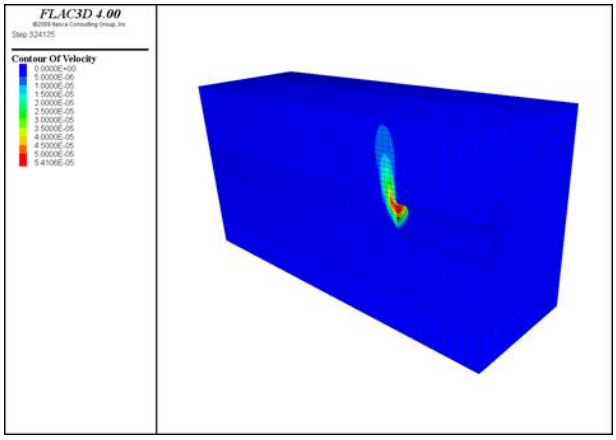

(a) Contour of velocity

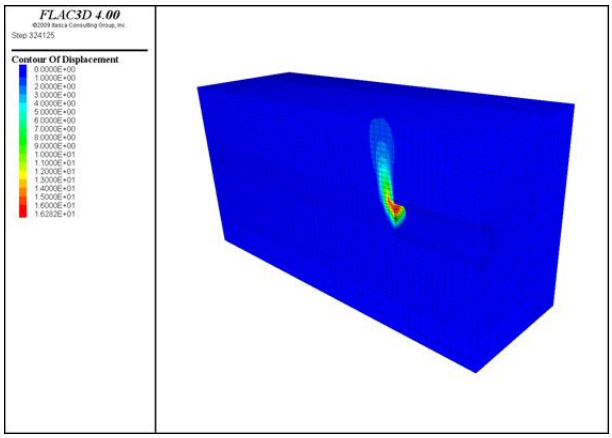

(b) Contour of displacement

Fig. 4 Calculation of tunnel collapse pressure without seepage

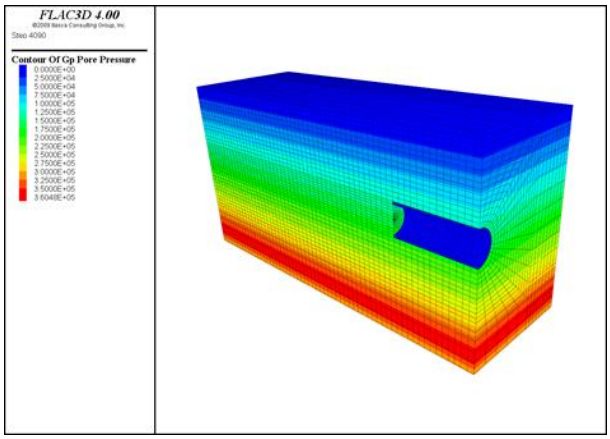

(a) Pore pressure distribution before tunnel excavation

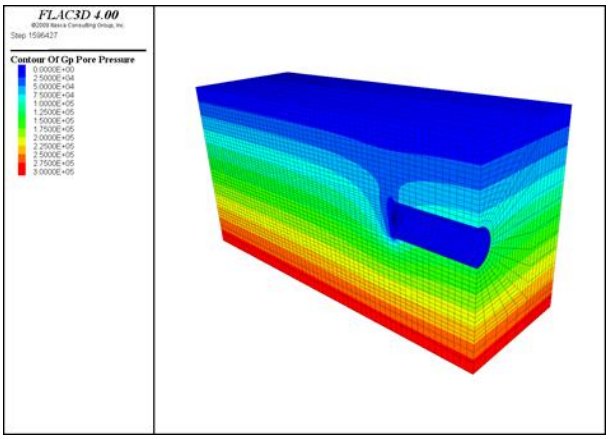

(b) Pore pressure distribution after tunnel excavation

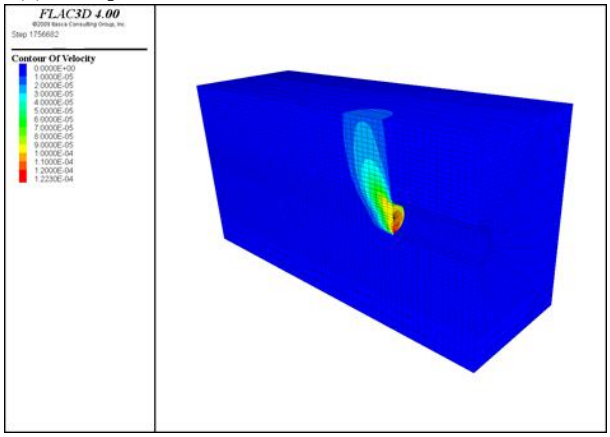

(c) Contour of velocity

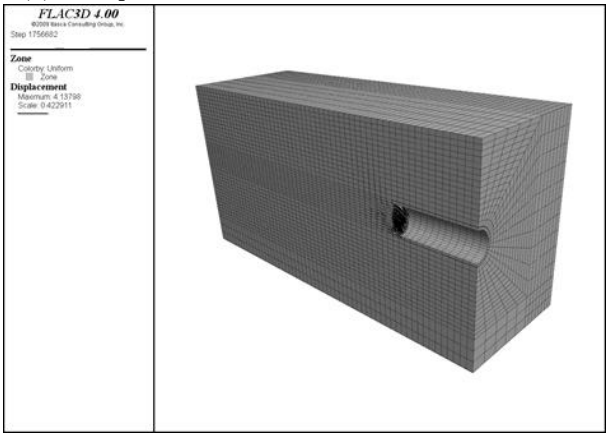

(d) Displacement vector

Fig. 5 Calculation of tunnel collapse pressure with seepage

applying the hydrostatic heads to the domain as an initial condition, the pressure heads at the wall and the face of the tunnel are taken to be zero in the drainage type while only those of the face are taken to be zero in the water-proof type. During tunnel construction below groundwater level, flow of groundwater into the tunnel leads to total head loss around tunnel, and causes the seepage pressure around the tunnel. Figs. 5(a) and 5(b) show the comparison in the pore pressure distribution between before and after tunnel excavation. Figs. 5(c) and 5(d) show the collapse velocity field with seepage pressure and the corresponding displacement vector at the time of failure. We can see that the location of a failure plane in front of the tunnel face is somewhat changed after the consideration of seepage effect.

The analyses are conducted for 40 cases of ground conditions as summarized in Table. 1. Each case involves analyses with both the drainage and the water-proof type for the seepage analysis.

Table 1 Cases of analysis for the calculation of the limiting collapse pressure

		c_0'									
		0	0.25	0.50	0.75	1.00	1.25	1.50	2.00	2.50	3.00
ρ	0	Case M01	Case M02	Case M03	Case M04	Case M05	Case M06	Case M07	Case M08	Case M09	Case M10
	1.00	Case M11	Case M12	Case M13	Case M14	Case M15	Case M16	Case M17	Case M18	Case M19	Case M20
	1.50	Case M21	Case M22	Case M23	Case M24	Case M25	Case M26	Case M27	Case M28	Case M29	Case M30
	2.00	Case M31	Case M32	Case M33	Case M34	Case M35	Case M36	Case M37	Case M38	Case M39	Case M40

Table 2 The calculation of the limiting collapse pressure by UBM (C=5 m, D= 5 m, H=5 m, i.e., C/D=1, H/D=1)

		c_0'									
		0	0.25	0.50	0.75	1.00	1.25	1.50	2.00	2.50	3.00
ρ	0	14.15	13.80	13.44	13.08	12.73	12.37	12.01	11.30	10.58	9.87
	1.00	14.15	11.85	9.54	7.23	4.93	2.62	0.31	−4.30	−8.92	−13.53
	1.50	14.14	10.87	7.59	4.31	1.03	−2.26	−5.54	−12.10	−18.67	−25.23
	2.00	14.14	9.90	5.64	1.38	−2.87	−7.13	−11.39	−19.90	−28.42	−36.93

Table 3 The calculation of the limiting collapse pressure by UBM (C=10 m, D= 5 m, H=10 m, i.e., C/D=2, H/D=2)

		c_0'									
		0	0.25	0.50	0.75	1.00	1.25	1.50	2.00	2.50	3.00
ρ	0	17.29	16.93	16.58	16.22	15.86	15.51	15.15	14.43	13.72	13.01
	1.00	17.28	13.77	10.25	6.73	3.21	−0.30	−3.82	−10.86	−17.90	−24.94
	1.50	17.27	12.19	7.09	1.99	−3.11	−8.21	−13.31	−23.51	−33.71	−43.91
	2.00	17.26	10.61	3.93	−2.75	−9.43	−16.11	−22.79	−36.16	−49.52	−62.88

2.3 Comparison with UBM solution

The various analysis cases are designed to understand the effect of strength increase with depth. The parameter ranges are chosen after considering the acceptable field condition. The limiting collapse pressures by UBM for various cases are calculated as summarized in Table 2 and Table 3. When the depth-dependent rate of change (represented as ρ) of effective cohesion increases, the required face supporting pressure decreases. The negative limiting collapse pressure values in both tables indicate that additional face supporting pressure is unnecessary to ensure the stability of the tunnel face.

3. Probabilistic model formulation

A probabilistic model to predict the limiting collapse pressure of tunnel face can be written as

$$\sigma_T(\boldsymbol{X}) = \hat{\sigma}_T(\boldsymbol{X}) + \gamma(\boldsymbol{X}) + s\varepsilon \tag{11}$$

where, σ_T =the limiting collapse pressure by the FLAC^{3D}, $\hat{\sigma}_T$ =the limiting collapse pressure by the upper bound theorem is defined in Eq. (1), $\boldsymbol{X} = (\alpha, \beta, k_1, k_2, c_0', \emptyset', \rho, \gamma, C, D, \sigma_S, \sigma_{S.F.})$ =the random variables, $\gamma(\boldsymbol{X})$ =the correction term for the bias inherent in the deterministic model that is expressed as a function of the variables $\boldsymbol{X}$, $s\varepsilon$ =the model error, s =the unknown standard deviation of the model error, ε = a random variable with zero mean and unit variance of standard normal distribution. In assessing the probabilistic model, the following assumptions are made: (a) the model variance σ^2 is independent of $\boldsymbol{X}$ (homoskedasticity assumption), and (b) ε follows the normal distribution (normality assumption). These assumptions are verified by using diagnostic plots of the data or the residuals versus the model predictions. After reviewing the diagnostic plot of the residuals as shown in Fig. 6(a), it is introduced the constant correction term that is independent of the random variables, $\gamma(\boldsymbol{X})$ =0.075, to remove potential bias in the model. The normality assumption is also checked in the Q-Q normal plot of the residuals as shown in Fig. 6(b). Fig. 7 shows the comparison in the limiting collapse pressure between by UBM solutions and FLAC^{3D} numerical models.

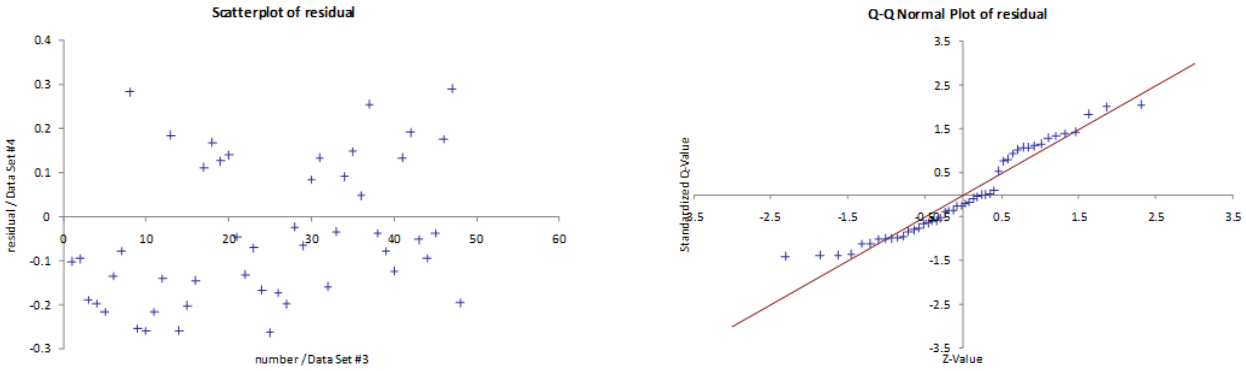

(a) Diagnostic plot (b) Q-Q normal plot

Fig. 6 Residual analysis

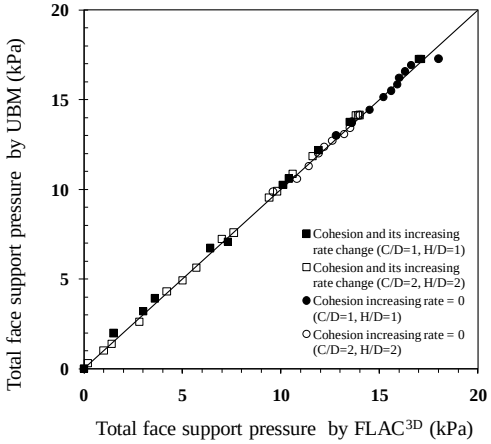

Fig. 7 Comparison in the limiting collapse pressure between UBM and FLAC^{3D} numerical models

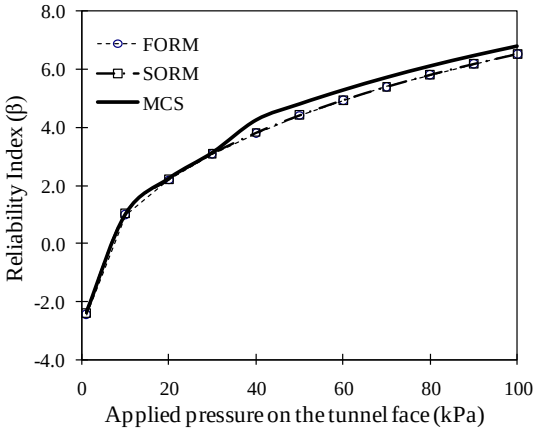

Fig. 8 Reliability index for the different applied pressure values

4. Reliability analysis

The limit state function, $g(\boldsymbol{X})$, with respect to the collapse of tunnel face in the ultimate limit state (ULS) can be described as

$$g(\boldsymbol{X}) = \sigma_{applied} - \sigma_T(\boldsymbol{X}) \tag{12}$$

where, $\sigma_{applied}$ = the applied pressure on the tunnel face and $\sigma_T(\boldsymbol{X})$ =the limiting collapse pressure calculated by the FLAC^{3D} as described in the previous section.

When a probabilistic stability analysis is conducted, the failure probability for the tunnel face collapse can be defined as

$$p_f = P[g(\boldsymbol{X}) \le 0] = \int_{g(\boldsymbol{X})\le 0} f(\boldsymbol{X})d\boldsymbol{X} \tag{13}$$

where, $f(\boldsymbol{X})$ is the joint probability density function of the basic variable vectors $\boldsymbol{X} = (\alpha, \beta, k_1, k_2, c_0', \emptyset', \rho, \gamma, C, D, \sigma_S, \sigma_{S.F.})$. The reliability analyses using first-order reliability method (FORM), the second-order reliability method (SORM), and Monte Carlo simulations (MCS) are performed based on the parameters summarized in Table 4. In this case, some of the parameters $(C, D, \sigma_S, \sigma_{S.F.})$ are assumed to be constant values.

Table 4 Parameters for the reliability analysis

Parameter ranges	Distribution models	Mean	COV*
$0 < c_0' < \infty$	Lognormal	1.00	0.20
$0 < \emptyset' < \infty$	Lognormal	35.0	0.20
$0 < \rho < \infty$	Lognormal	0.50	0.20
$0 < \gamma < \infty$	Lognormal	15.2	0.20

$C = 10.0m, D = 5.0m,$
$\sigma_S = 10kN/m^2$ $\sigma_{S.F.} = 34.9kN/m^2$
*COV= coefficient of variation=standard deviation/mean

The reliability index for the different applied pressure values can be obtained as shown in Fig. 8. As the applied pressure on the tunnel face increase, the reliability index also increases and it also means that the probability of failure will decrease.

5. Sensitivity and importance measures

In a reliability analysis, sensitivity measures are used to determine the effects on the reliability of changes in the parameters in the limit state function or in the distribution of the random variables. Fig. 9 shows the sensitivity

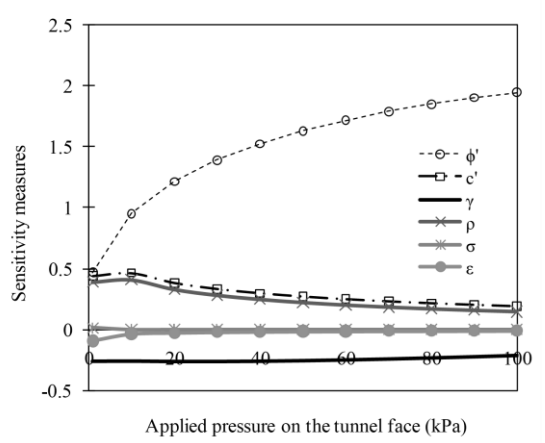

Fig. 9 Sensitivity measures for the random variables

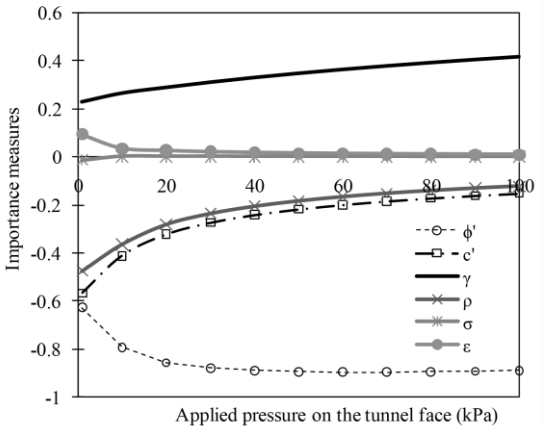

Fig. 10 Importance measures for the random variables

measures as a function of the applied pressure on the tunnel face. It is observed that $\emptyset'$ has larger effects on the reliability. As the applied pressure increases, the tunnel face stability is most sensitive to $\emptyset'$. Fig. 10 shows the importance measures of all random variables for the tunnel face stability. Observations similar to those made for the sensitivity analysis can be made for the importance measures. The positive signs of the importance measures indicate that these are "load" (demand) variables. The negative sign of the importance measure indicates that this random variable acts as a "resistance" (capacity) variable in the limit state function. It can be seen that $\emptyset'$ is the most important variable and γ is the second most important variable.

5. Conclusions

The settlement profiles in shallow tunnel construction in an urban area are mainly affected by the face stability. Face stability analysis provides the most probable failure mechanisms and the understanding about parameters that need to be considered for the evaluation of ground movements caused by tunneling. The limiting tunnel collapse pressure in a Mohr-Coulomb (c', ∅') soil from the upper bound method (UBM) of limit analysis theory which can consider the effect of seepage into the tunnel face and strength increase with depth.

The influence of seepage forces and depth-dependent effective cohesion is investigated for a dual-cone failure mechanism using the UBM implemented by numerical analysis. The upper bound analytical derivation for depth-dependent effective cohesion and corresponding numerical results are presented and compared to those presented by previous authors. In addition, the numerical analysis demonstrated the influence of tunnel diameter on required face supporting pressure.

After the UBM solution is verified with the numerical experiments, the probabilistic model is proposed to calculate the unbiased limiting tunnel collapse pressure. A reliability analysis of a shallow circular tunnel driven by a pressurized shield in a frictional and cohesive soil is presented to consider the inherent uncertainty in the input parameters and the proposed model. The ultimate limit state (ULS) for the face stability is considered in the analysis. The probability of failure that exceeding a specified applied pressure at the tunnel face is estimated. Sensitivity and importance measures are computed to identify the key parameters and random variables in the model.

References

Atkinson, J.H. and Potts, D.M. (1977), "Stability of a shallow circular tunnel in cohesionless soil", *Géotechnique*, **27**(2), 203-215. https://doi.org/10.1680/geot.1977.27.2.203.

Chambon, P. and Corte, J.F. (1994), "Shallow tunnels in cohesionless soil: Stability of tunnel face", *J. Geotech. Eng.*, **120**(7), 1148-1165. https://doi.org/10.1061/(ASCE)0733-9410(1994)120:7(1148).

Davis, E.H., Gunn, M.J., Mair, R.J. and Seneviratne, H.N. (1980), "The stability of shallow tunnels and underground openings in cohesive material", *Géotechnique*, **30**(4), 397-416. https://doi.org/10.1680/geot.1980.30.4.397.

Eclaircy-Caudron, S., Dias, D. and Kastner, R. (2007), "Assessment of soil parameters met during a tunnel excavation: Use of inverse analysis on in situ measurements---Case of Bois de Peu (France)", Advances in Measurement and Modeling of Soil Behavior (GSP 173), ASCE, Denver, CO, 1-10.

FLAC^{3D} (2009), Fast Lagrangian Analysis of Continua in 3 Dimensions. ITASCA Consulting Group, Inc., Minneapolis, Minnesota.

Huang, F., Wang, D., Xiao, N. and Ou, R.C. (2021), "Upper bound limit analysis of blow-out failure mode of excavation face of shield tunnel considering groundwater seepage", *Geomech. Eng.*, **26**(3), 227-234. https://doi.org/10.12989/gae.2021.26.3.227.

Jardine, R.J., Potts, D.M., Fourie, A.B. and Burland, J.B. (1986), "Studies of the influence of non-linear stress strain characteristics in soil-structure interaction", *Géotechnique*, **36**(3), 377-396. https://doi.org/10.1680/geot.1986.36.3.377.

Khezri, N., Mohamad, H. and Fatahi, B. (2016), "Stability assessment of tunnel face in a layered soil using upper bound theorem of limit analysis", *Geomech. Eng.*, **11**(4), 471-492. https://doi.org/10.12989/gae.2016.11.4.471.

Leca, E. and Dormieux, L. (1990), "Upper and lower bound solutions for the face stability of shallow circular tunnels in frictional material", *Géotechnique*, **40**(4), 581-606. https://doi.org/10.1680/geot.1990.40.4.581.

Li, B., Fu, Y., Hong, Y. and Cao, Z. (2021), "Deterministic and

probabilistic analysis of tunnel face stability using support vector machine", *Geomech. Eng.*, **25**(1), 17-30. https://doi.org/10.12989/gae.2021.25.1.017.

Mollon, G., Dias, D. and Soubra, A.H. (2009), "Probabilistic analysis of circular tunnels in homogeneous soil using response surface methodology", *J. Geotech. Geoenviron. Eng.*, **135**(9), 1314-1325. https://doi.org/10.1061/(ASCE)GT.1943-5606.0000060.

Mroueh, H. and Shahrour, I. (2003), "A full 3-D finite element analysis of tunneling-adjacent structures interaction", *Comput. Geotech.*, **30**(3), 245-253. https://doi.org/10.1016/S0266-352X(02)00047-2.

Pan, Q., Chen, Z., Wu, Y., Dias, D. and Oreste, P. (2021), "Probabilistic tunnel face stability analysis: A comparison between LEM and LAM", *Geomech. Eng.*, **24**(4), 399-406. https://doi.org/10.12989/gae.2021.24.4.399.

Park, J.K. (2011), Adaptive Reliability Analysis of Excavation Problems. Doctoral dissertation, Texas A&M University, College Station.

Wong, H., Subrin, D. and Dias, D. (2006), "Convergence-confinement analysis of a bolt-supported tunnel using the homogenization method", *Can. Geotech. J.*, **43**(5), 462-483. https://doi.org/10.1139/t06-016.

Yoo, C. (2002), "Finite-element analysis of tunnel face reinforced by longitudinal pipes", *Comput. Geotech.*, **29**(1), 73-94. https://doi.org/10.1016/S0266-352X(01)00020-9.

Zhang, B., Jiang, J., Zhang, D. and Liu, Z. (2021), "Upper bound solution of collapse pressure and permanent displacement of 3D tunnel faces using the pseudo-dynamic method and the kinematic approach", *Geomech. Eng.*, **25**(6), 521–533. https://doi.org/10.12989/gae.2021.25.6.521.

Zhou, B., Sue, Y., Li, S., Qiu, D., Tao, Y., Zhang, K., Zhang, X. and Xia, T. (2020), "Probabilistic analysis of tunnel collapse: Bayesian method for detecting change points", *Geomech. Eng.*, **22**(4), 291-303. https://doi.org/10.12989/gae.2020.22.4.291.